JOURNAL OF MATERIALS SCIENCE **35** (2000) 3931–3937

Strengthening of alumina by cerium-zirconate ($Ce_2Zr_2O_7$)

A. SAHA, D. C. AGRAWAL
Materials Science Programme, I.I.T Kanpur, Kanpur 208016, India

Composite powders of Al_2O_3 and 0 to 30 vol% $Ce_2Zr_2O_7$ are prepared by a hybrid sol-gel method using Al_2O_3 powders and a sol formed from Zr-alkoxide and cerium nitrate. All the Zr from the sol goes to form the cerium zirconate phase when the powders are calcined in N_2. Pressureless sintering in air at 1500°C yields composites with high density (∼98%). Maximum values of fracture toughness and strength, 6.5 MPa $\sqrt{m}$ and 620 MPa respectively, (e.g. 3.5 MPa $\sqrt{m}$ and 350 MPa for pure Al_2O_3) are obtained in 10 vol% $Ce_2Zr_2O_7$ composite sintered in air. The dominant mechanism for enhancement in K_{IC} is believed to be crack bridging. Crack bridging activity in the 10 vol% composite is found to be maximum and extends upto ∼190 μm from the crack tip.

1. Introduction

Fracture toughness (K_{IC}) and strength (σ_f) of ceramics can be enhanced in many cases by incorporation of a reinforcement in the form of particles [1–4], whiskers [5–7], platelets [8], fibres [9] etc. Many such studies have been carried out on alumina. The K_{IC} and σ_f for unreinforced alumina prepared by pressureless sintering are approximately 3.5 MPa $\sqrt{m}$ and 250 MPa respectively [10]. These can be improved to varying degrees by inclusion of tetragonal (t) zirconia particles [1], SiC whiskers [5–7] and particles of TiC, B_4C etc [3, 4]. Some of the data is summarized in Table I.

Preparation of Al_2O_3-ZrO_2 composites can be carried out using pressureless sintering with substantial improvement in properties. The preparation of ceramic composites, other than Al_2O_3-ZrO_3 composites, generally requires hot pressing or hot isostatic pressing which makes these materials expensive and less versatile. In case of Al_2O_3-ZrO_2 composites, careful mixing of constituent powders to ensure a uniform dispersion of unagglomerated ZrO_2 is needed. Furthermore, the improvement in properties is lost at higher temperature because the stress induced t → m (monoclinic) transformation of ZrO_2, which is mainly responsibe for improved K_{IC}, becomes increasingly difficult with increasing temperature. The low temperature aging [11] also induces t → m transformation and leads to degradation in K_{IC}. A reinforcement material for alumina and other ceramics which allows easy processing and is not very sensitive to environment and temperature is therefore desirable.

One of the additives used to stabilize the t phase in ZrO_2 is CeO_2. It forms tetragonal solid solution with ZrO_2 in amounts upto 20 mol%, although a significant discrepency exists on the solubility limit of CeO_2 in t-ZrO_2 [12–14]. In an earlier work by us, the strength and toughness of samples of Al_2O_3-(Ce)ZrO_2 composites were found to give different values depending on their location in the sintered pellets. The samples taken from the interior of the sintered pellets (Set II) had in general better mechanical properties than those taken from the near surface regions (Fig. 1). The samples from the interior were found to contain $Ce_2Zr_2O_7$, a phase with cubic structure which contains Ce in Ce^{3+} state and forms in an inert or reducing atmosphere [15, 16]. In the present work therefore we have studied the effect of this non-transforming cerium zirconate phase ($Ce_2Zr_2O_7$) on the mechanical properties of Al_2O_3. The zirconate phase is prepared by co-precipitation of Ce and Zr hydroxides followed by calcination in N_2. Composites of Al_2O_3 and $Ce_2Zr_2O_7$ are frabricated to high density (∼98%) by pressureless sintering. Enhanced properties superior to those of many other Al_2O_3 composites are obtained. Crack bridging is shown to be an important mechanism in these composites and is believed to be the dominant mechanism contributing to enhancement in K_{IC}.

2. Experimental

Composites of Al_2O_3 and $Ce_2Zr_2O_7$ containing 5, 10, 20 and 30 vol% zirconate are prepared by a hybrid sol-gel method [17]. First a sol containing Ce and Zr in molar ratio 1 : 1 is prepared by dissolving $Ce(NO_3)_3.6H_2O$ in triple distilled water followed by dropwise addition of zirconium *n*-propoxice (Zr-*n*-p) to it. A white precipitate is formed which is dissolved by dropwise addition of nitric acid (HNO_3) while stirring. Calculated amount of Al_2O_3 powder is added to the sol and the slurry is ultrasonicated to break-up the Al_2O_3 agglomerates. The slurry is then added drop by drop to sufficient quantity of an aquous NH_4OH solution of pH 10.5 to ensure complete coprecipitation of Ce and Zr hydroxides. The pH of the mixture is adjusted to 10.5 by further

TABLE I Mechanical properties of some alumina based composites

Sl.No	Material	K_{IC} (MPa $\sqrt{m}$)	σ_f (MPa)	Ref.
1	Al_2O_3 + 40 vol% t-ZrO_2	12	900	1
2	Al_2O_3 + 15 vol% m-ZrO_2	10	480	24
3	Al_2O_3 + 5 vol% B_4C	5.2	570	4
4	Al_2O_3 + 30 vol% TiC	6.2	635	3
5	Al_2O_3 + 30 vol% SiC whisker	9.5	650	6
6	Al_2O_3 + 20 vol% SiC whisker	9	800	7

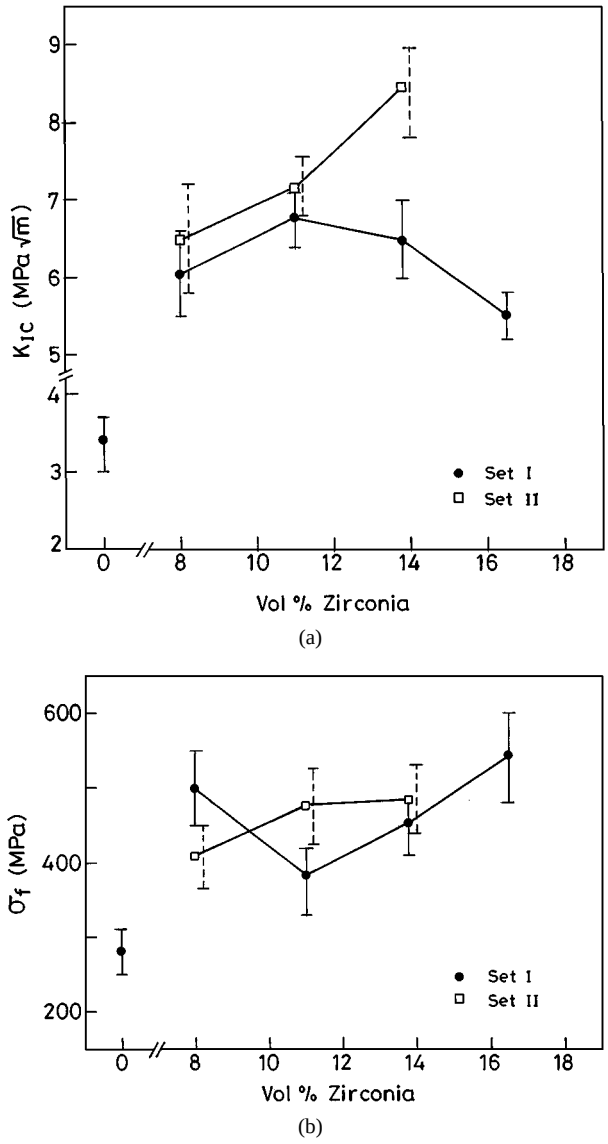

Figure 1 Mechanical properties of Al_2O_3-ZrO_2 composites with (Set II) and without (Set I) $Ce_2Zr_2O_7$ phase; (a) fracture toughness and (b) fracture strength. Data points for Set II samples have been shown by broken lines and shifted slightly to the right for clarity.

addition of NH_4OH. After stirring for 2 h, the suspension is allowed to settle. The precipitate is then washed with triple distilled water followed by propanol to remove ammonia and to prevent agglomeration during drying [18] respectively. The precipitate is oven dried at

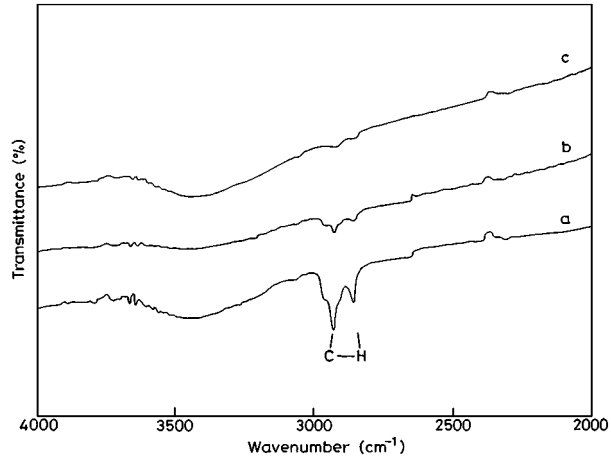

Figure 2 Infra red (IR) spectra of $Ce_2Zr_2O_7$ powders calcined in N_2 (a) after calcination, (b) after further annealing in air at 500°C for 2 h and (c) after annealing in air at 500°C for 2.5 h.

100°C, crushed lightly and sieved through 70–80 mesh and subsequently calcined at 1000°C for 3 h in N_2. IR spectrum of this powder shows a peak corresponding to -C-H- streching indicating that the carbon from the residual organics is not completely removed by calcination (Fig. 2a). Fig 2b and c show the results of further calcination of this powder in air at 500°C for 2 h and 2.5 h respectively. The -C-H- peak disappears after 2.5 h treatment. Hence in most cases the powder is subjected to a second calcination in air at 500°C for 3 h to remove the residual organics. The calcined powder is ball milled for 8 h using propanol with alumina balls. The powder is mixed with PVA solution as binder so as to yield 1 wt% PVA in the powders and subsequently pressed in a steel die into 20 mm × 7 mm × 2.2–3.6 mm bars at a pressure of 300 MPa and sintered at 1500°C for 3 h in N_2 or in air.

The sintered density of the samples is measured by Archimedes method. The phases in the calcined powder and in the sintered bars are determined by X-ray diffraction (XRD) using X-ray diffractometer (Reich Seifert Isodebyeflex 2002, Germany) with Ni filtered Cu K_α radiation. Rectangular bars having dimension 1.2 mm × 1.8 mm × 15 mm are cut and polished to 1 μm finish using diamond paste. These are tested in 3 point bending with span length of 7 mm for determining the fracture strength (σ_f). Fracture toughness (K_{IC}) is measured by single edge notch beam (SENB) technique in 3 point bending on polished samples having dimension 1 mm × 3 mm × 15 mm. The notch depth is half of the sample depth.

For microstructural observation, the samples are polished and thermally etched at 1320°C for 30 minutes. They are observed in a scanning electron microscope (Model JSM 840A, JEOL, Japan). The diameter of $Ce_2Zr_2O_7$ grains is calculated as the diameter corresponding to the circle of equavalent area. Stereological conversion for grain size distribution from 2 dimensional (2D) planar surface to representative 3D distribution is done [19]. The average grain size of zirconate is calculated from the distribution. The average grain size of Al_2O_3 is measured by mean intercept length method taking about 300 grains. A multiplying factor

of 1.56 is used and correction is made for zirconate second phase [20]. Cracks produced on the polished surfaces of the composites by indenting with a vicker indentor at a load of 30–40 Kg are observed.

3. Results

Fig. 3 shows the XRD plot of the calcined powder and the composites sintered in N_2 and in air. Zirconia is present in the calcined powder (with or without air annealing) only as a $Ce_2Zr_2O_7$ phase (Fig. 3a). In the air sintered samples, in addition to the zirconate phase, a small amount of ZrO_2 (t′ or c) is also present (which does not undergo any phase transformation during fracture) (Fig. 3b). Air annealing of calcined powders does not alter the relative amounts of the two phases after sintering in air. The samples sintered in N_2 show only the zirconate phase with traces of AlN phase (Figs 3c and 4 respectively).

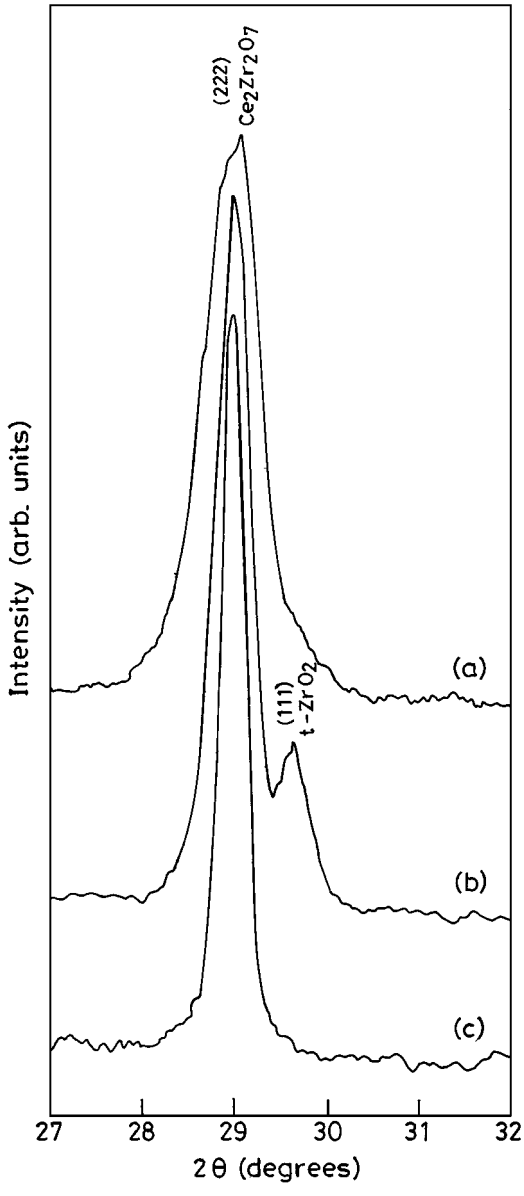

Figure 3 X-ray diffractograms of Al_2O_3-20 vol% $Ce_2Zr_2O_7$ (a) powders after calcination in N_2 and annealing in air at 500°C for 3 h, (b) powders treated as in (a) and sintered in air (NAA), and (c) powders calcined in N_2 and sintered in N_2 (NN).

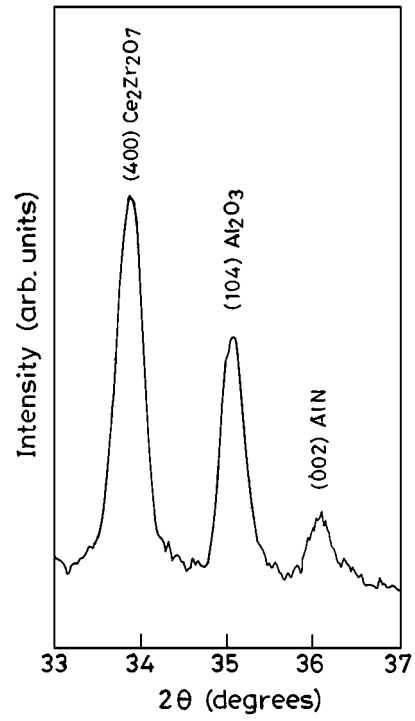

Figure 4 X-ray diffractogram of sintered surface of composite containing 20 vol% $Ce_2Zr_2O_7$ sintered in N_2 (NN).

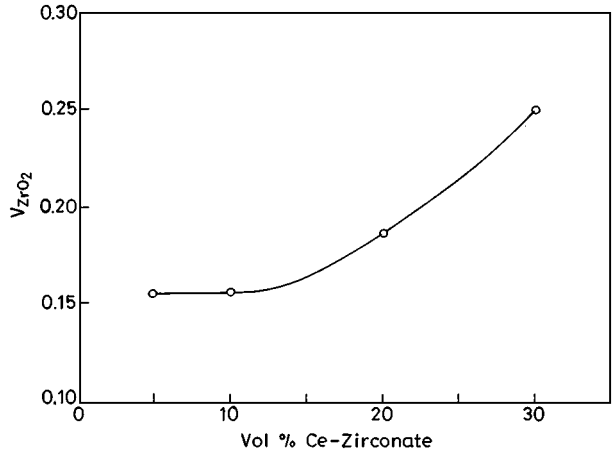

Figure 5 Fraction of ZrO_2 (V_{ZrO_2}) vs vol% $Ce_2Zr_2O_7$ in the air annealed air sintered (NAA) samples.

The fraction of ZrO_2 (V_{ZrO_2}) in the air sintered samples is estimated using the relation,

$$V_{ZrO_2} = \frac{I_{t(111)}}{I_{t(111)} + I_{CeZ(222)}}$$

where $I_{t(hkl)}$ and $I_{Cez(hkl)}$ are the intensities of the (hkl) lines of tetragonal ZrO_2 and the cerium zirconate phase respectively. V_{ZrO_2} remains constant upto 15 vol% zirconate (nominal) after which a slow increase is observed (Fig. 5).

Fig. 6 shows the change in density, ρ, with vol% $Ce_2Zr_2O_7$. It is seen that $\rho_{NAA} > \rho_{NA} > \rho_{NN}$ where NAA indicates calcination in N_2 followed by annealing and sintering in air, NA indicates calcination in N_2 and sintering in air and NN indicates both calcination and sintering in N_2. The relative density has been calculated assuming that the samples contain Al_2O_2 and

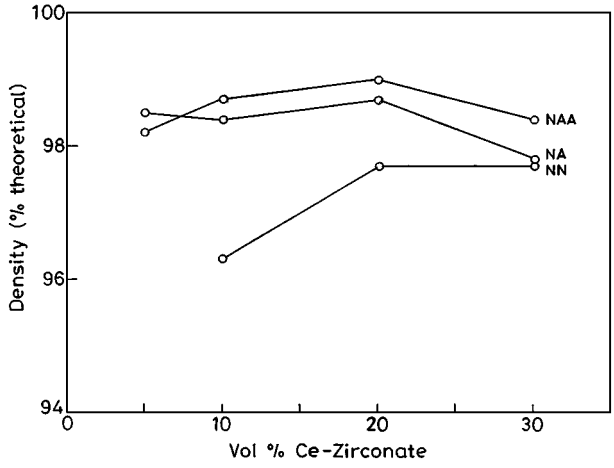

Figure 6 Density of sintered samples vs volume% $Ce_2Zr_2O_7$.

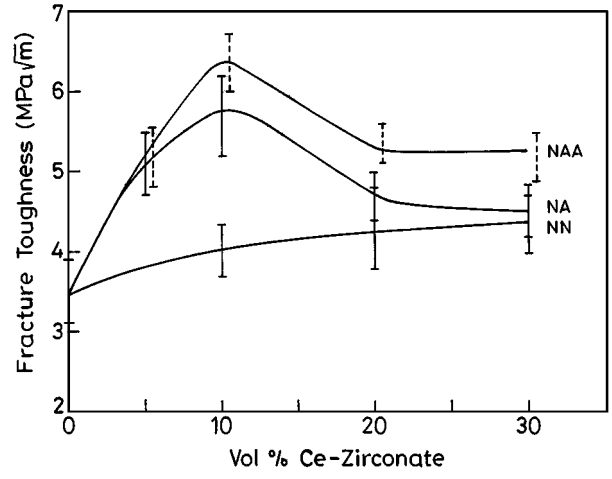

Figure 7 Fracture toughness vs vol% $Ce_2Zr_2O_7$. Data points for air annealed/air sintered (NAA) samples have been shown by broken lines and shifted slightly to the right for clarity.

$Ce_2Zr_2O_7$ phases in the amounts initially used; this may not be strictly correct, specially for the NAA samples, as discussed later. However, the error due to this is not likely to be large. A high density (>96%) is obtained in both air and N_2 sintered samples.

In N_2 sintered samples, the K_{IC} increases slowly with the addition of zirconate from 3.5 MPa $\sqrt{m}$ for Al_2O_3 to a maximum value of 4.3 MPa $\sqrt{m}$ for 30 vol% zirconate (Fig. 7). The improvement in K_{IC} is more dramatic in the air sintered samples where a peak in K_{IC} occurs at 10 vol% zirconate, the maximum K_{IC} of 6.5 MPa $\sqrt{m}$ being obtained in the air annealed, air sintered (NAA) samples (Fig. 7).

The trends in the fracture strength (σ_f) are similar to K_{IC}, with maximum values being obtained in the air annealed/air sintered (NAA) samples. The maxima are flatter, extending from 5 to 20 vol% zirconate (Fig. 8). Maximum strength obtained is ~620 MPa. Strength and toughness intermediate between N_2 sintered (NN) and air annealed/air sintered (NAA) samples are obtained when the powders are not air annealed prior to sintering in air (Figs 7 and 8).

4. Discussion

In the present investigation, Ce-zirconate of composition $Ce_2Zr_2O_7$ is intended to be prepared. This phase

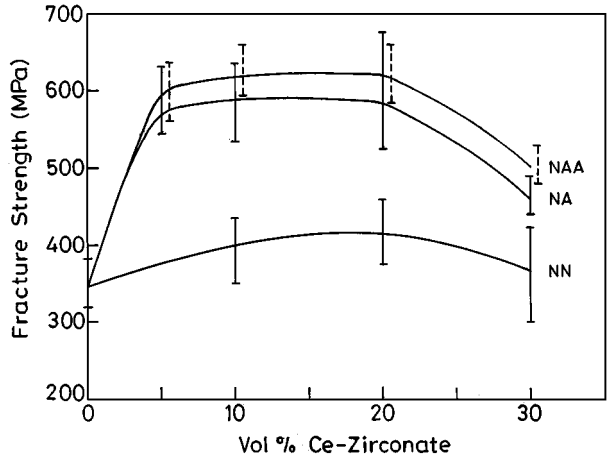

Figure 8 Fracture strength vs vol% $Ce_2Zr_2O_7$. Data points for air annealed/air sintered (NAA) samples have been shown by broken lines and shifted slightly to the right for clarity.

has been observed to form when Ce ions are in 3+ valence state under reducing ambient. Sintering in air ambient may change the stoichiometry of this phase and may also lead to the formation of other phases such as $Ce_{.75}Zr_{.25}O_2$ [21]. Since the XRD peaks of $Ce_2Zr_2O_7$ and $Ce_{.75}Zr_{.25}O_2$ phases overlap, it is difficult to determine the respective amounts of these phases. However, the formation of $Ce_{.75}Zr_{.25}O_2$ or a change in the stoichiometry of $Ce_2Zr_2O_7$ such that some Ce^{3+} changes to Ce^{4+} and replaces Zr^{4+} in it, would be consistent with the formation of some ZrO_2 (t′ or c), which is observed in the air sintered samples.

Incorporation of the non-tranforming zirconate phase is found to be very effective in enhancing the mechanical properties of Al_2O_3 as shown in Figs 7 and 8. The best properties are obtained in the air sintered samples from powders calcined in N_2 and subsequently annealed in air.

Some of the primary toughening mechanisms possible in the non-transforming particulate reinforced ceremics are a) crack deflection [22], b) crack bridging [23], c) microcracking [24] and d) residual stress (strain) field due to mismatch between the coefficients of thermal expansion (CTE) of the ceramic matrix and the particulate [25]. According to the model of Faber and Evans [22] the enahancement in toughness due to crack deflection should be in the range of 12 to 15% for uniformly distributed particles having volume fraction of 0.1 to 0.3. Clearly an enhancement in K_{IC} by >85% in our 10 vol% zirconate-Al_2O_3 samples is not likely to be solely due to crack deflection although in several systems enhancement in toughness as high as 40 to 70% has been attributed to crack deflection [2, 26–28]. Increase in K_{IC} due solely to the change in fracture mode from intergranular to transgranular has been estimated to be 58% [29]. Niihara *et al*. [2] have attributed the improvement in fracture toughness by 40% in Al_2O_3 containing SiC particles to this change in fracture mode. Hanssen *et al*. [29] have found the K_{IC} of hot pressed Al_2O_3 and Al_2O_3-33 vol% SiC whiskers composites to be 4 MPa $\sqrt{m}$ and 5 to 8 MPa $\sqrt{m}$ respectively and have proposed crack deflection in combination with change in fracture mode as an explanation for this increase.

No evidence of any crack bridging was found in their samples.

Toughening by crack bridging is well known for pure Al_2O_3 [30], Si_3N_4 [31] and other non-transforming ceramic composites [32]. Swanson *et al.* [30] convincingly demonstrated that the crack growth resistance in Al_2O_3 increases with crack extension due to localized grain bridging. Padture *et al.* [32] studied the effect of volume fraction and the particle size of the second phase on toughness in Al_2O_3-Al_2TiO_5 system and showed that addition of a second phase below a certain limit can improve the flaw tolerance behaviour well beyond any law of mixture by enhancing the effectiveness and density of the bridges. He also observed that beyond a critical composition, the strength is severely degraded indicative of microcrack coalescence. Homney *et al.* [6] found that the addition of 30 vol% SiC whisker increases the strength and toughness to 650 MPa and 9.5 MPa $\sqrt{m}$ respectively (vs 385 MPa and 5 MPa $\sqrt{m}$ for pure Al_2O_3). Better properties are reported by Wie and Becher [7] in Al_2O_3-SiC whisker composites containing 20 vol% SiC whisker where K_{IC} and σ_f are found to be 9 MPa $\sqrt{m}$ and 800 MPa respectively (vs 4.5 MPa $\sqrt{m}$ and 350 MPa for pure Al_2O_3). For both the cases the enhancement in properties is attributed to fibre bridging and crack deflection.

In our samples also, we believe that the major contribution to enhanced toughness is due to crack bridging. Clear evidence of crack bridging is obtained in the indentation produced cracks as discussed below:

Fig. 9 shows the cracks produced by indentation in Al_2O_3 and Al_2O_3-10 vol% $Ce_2Zr_2O_7$. No crack bridging is seen in zirconate free alumina sample (Fig. 9a). On the other hand, several crack bridging sites can be seen in the Al_2O_3-10 vol% $Ce_2Zr_2O_7$ samples (Fig. 9b–d). The crack bridging activity is continuous upto $\geq$190 μm from the crack tip (Fig. 9d). Swanson *et al.* [30] have also found that crack bridging by grains continues to persist at distances as large as 100 grain diameters from the crack tip.

In 5 vol% $Ce_2Zr_2O_7$ samples, the crack bridging activity is much less and observed only near the crack tip (Fig. 10a). Crack bridges are conspicuously absent at a distance $\geq$90 μm from the crack tip (Fig. 10b). In the 30 vol% $Ce_2Zr_2O_7$ samples the crack passes through the specimen causing clear separation between two parts without any crack bridging activity even near the crack tip (Fig. 10c). It appears that for crack bridging to occur, the grains should be large and simultaneously some residual stresses should be present. The grain size of Al_2O_3 decreases with increasing zirconate content (Table II). Thus at higher zirconate contents the extent of grain bridging should decrease as is observed for the 30 vol% $Ce_2Zr_2O_7$ samples. The residual stresses arise because of the difference in the coefficients of thermal expansion (CTE) between the different directions of the same crystal (Al_2O_3) or between the matrix and the reinforcing phase. The average CTE of Al_2O_3 is $8.43 \times 10^{-6}/^{\circ}C$ [33]. The CTE of zirconate is measured and found to be $12.2 \times 10^{-6}/^{\circ}C$ at 1056 K and is expected to be higher at higher temperature. Thus the introduction of $Ce_2Zr_2O_7$ is expected to introduce residual stresses in the composite. This appears to be

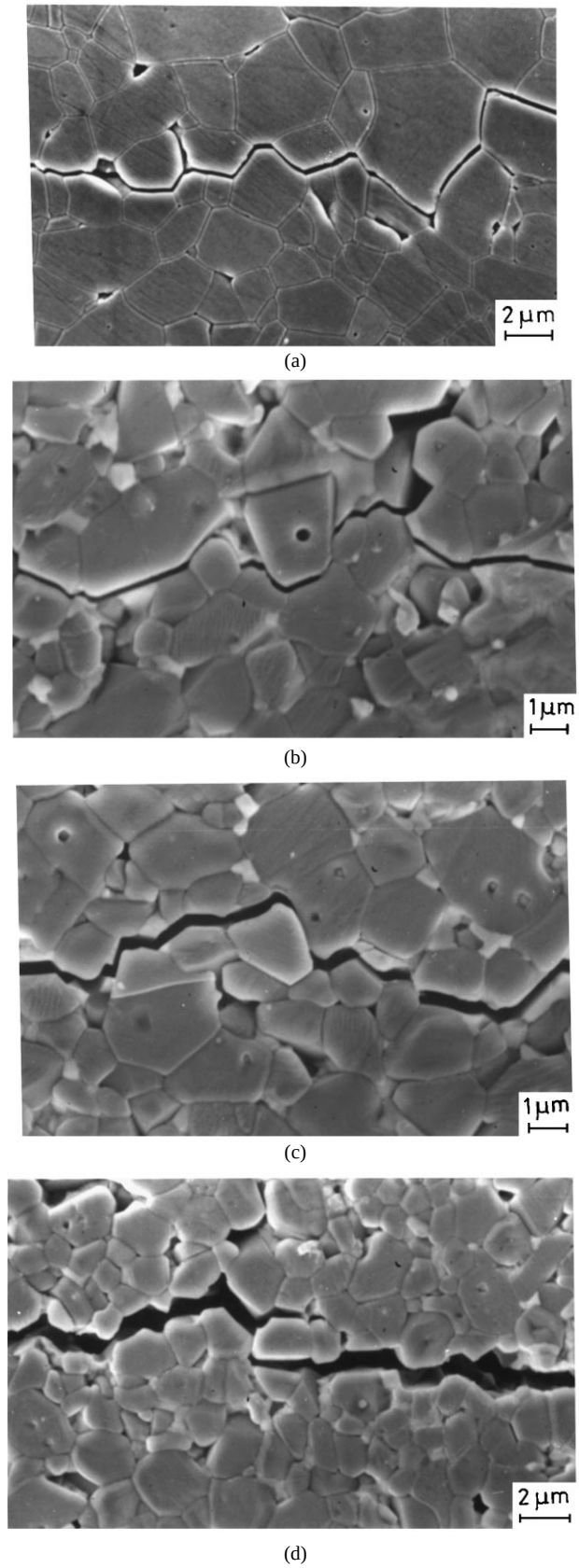

Figure 9 Indentation cracks in (a) zirconate free Al_2O_3 sample at a distance 60 μm from the crack tip, and in air annealed/air sintered (NAA) composite containing 10 vol% zirconate at a distance (b) 90 μm, (c) 120 μm and (d) 190 μm from the crack tip.

the reason for the increase in the grain bridging with initial addition of $Ce_2Zr_2O_7$ to Al_2O_3. At higher zirconate concentrations, in addition to a decrease in the grain size of Al_2O_3, the fraction of zirconate grains with much smaller grain size than Al_2O_3 becomes significant. The

TABLE II Grain sizes of Al_2O_3 and $Ce_2Zr_2O_7$

Volume% $Ce_2Zr_2O_7$	Grain Size of Al_2O_3 (μm)	Grain Size of $Ce_2Zr_2O_7$	
		$\bar{d}_{CeZ}$(μm)	σ_{CeZ}(μm)
0	3.2		
5	2.4	0.45	0.12
10	2.5	0.50	0.16
20	2.0	0.50	0.16
30	1.8	0.55	0.14

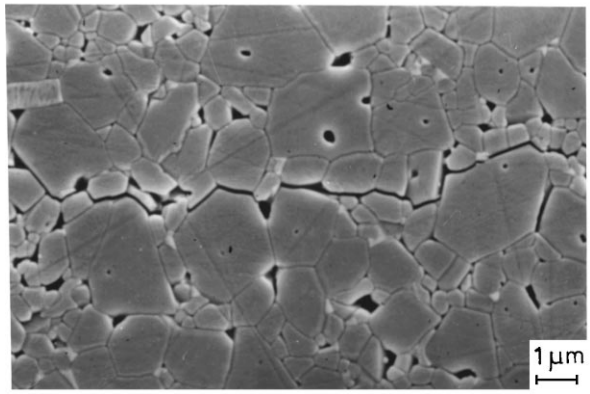

(a)

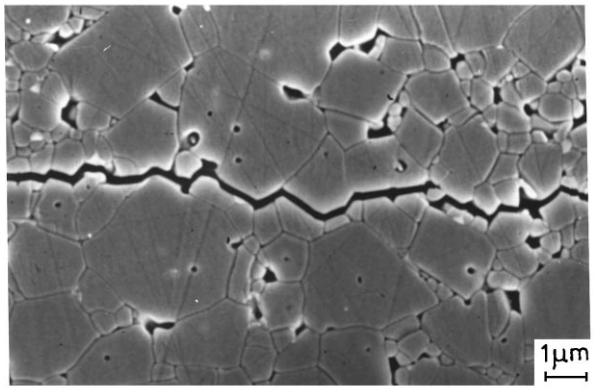

(b)

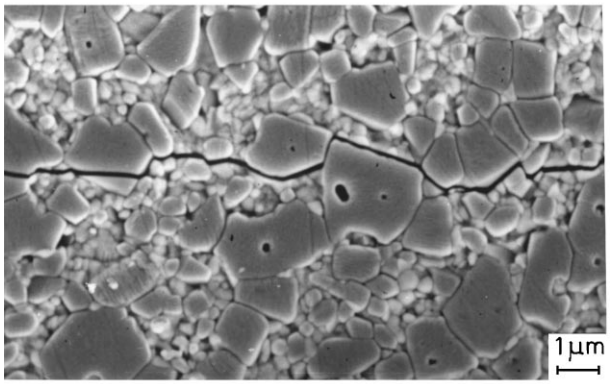

(c)

Figure 10 Indentation cracks in air annealed/air sintered (NAA) samples having different amounts of zirconate at different distances from the crack tip (a) 5 vol% zirconate, very near the crack tip, (b) 5 vol% zirconate, at 90 μm from the crack tip, (c) 30 vol% zirconate, very near the crack tip.

overall grain size is thus small and the grain bridging does not occur (Fig. 10c).

The strength of the composites increases with addition of the $Ce_2Zr_2O_7$ and remains constant when it contains 5–20 vol% zirconate even though there is a drop in fracture toughness at 20 vol%. This is not clearly

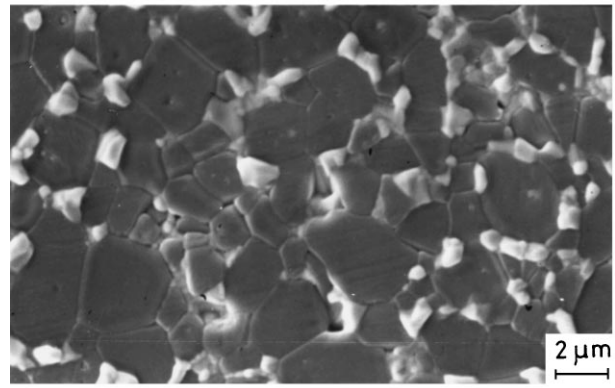

(a)

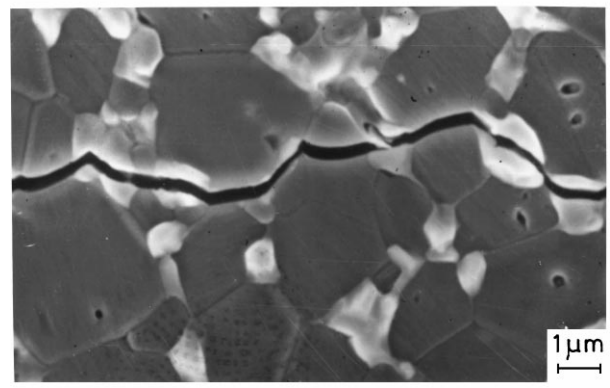

(b)

Figure 11 (a) Microstructure of the composite containing 10 vol% zirconate sintered in N_2 (NN), (b) Indentation crack in this composite.

understood. Such a behaviour has been observed in Si_3N_4-SiC composites also [34].

The mechanical properties of the N_2 sintered composites are found to be much inferior than those of the air sintered samples. Microstructure (Fig. 11a) reveals that $Ce_2Zr_2O_7$ phase is located at the Al_2O_3 grain junctions and completely fills the Al_2O_3 intergranular space. Its grain size is also larger (0.71 μm for 10 vol% zirconate). This shows that at the sintering temperature the surface energy of Al_2O_3-N_2 interfaces is more than that of the Al_2O_3-$Ce_2Zr_2O_7$ interface. The fracture occurs along the Al_2O_3 grain boundaries and through the zirconate grains (Fig. 11b). Thus the Al_2O_3-zirconate interface in this case is much stronger than zirconate. There is no evidence of any crack bridging. Lack of crack bridging, intergranular fracture and presence of small amount of AlN phase, all appear to contribute to the inferior mechanical properties of N_2 sintered samples.

Properties intermediate between N_2 sintered and the air annealed/air sintered samples are obtained when the powders are not calcined in air (Figs 7 and 8). This may be due to incomplete removal of carbon from alkoxide precursors during calcination.

5. Conclusion

Composites of Al_2O_3-$Ce_2Zr_2O_7$ can be prepared by starting from Al_2O_3 powders and a Zr-propoxide sol with dissolved $Ce(NO_3)_3.6H_2O$. The coprecipitated composite powder consists $Ce_2Zr_2O_7$ and Al_2O_3 after calcination in N_2 at 1000°C. Residual organics after calcination can be removed by annealing in air at 500°C.

The powders sinter to high density (upto ~98%) when sintered in air at 1500°C. Both K_{IC} and σ_f are enhanced upon addition of $Ce_2Zr_2O_7$. The properties are somewhat lower in composites in which residual organics are not removed or which are sintered in N_2. Improved mechanical properties in air sintered composites are believed to be due to crack bridging by the grains of the composites. The crack bridging is enhanced in larger grain size samples. The residual stresses produced due to thermal expansion mismatch between Al_2O_3 and $Ce_2Zr_2O_7$ are also believed to contribute to grain bridging.

Highest values of K_{IC} (6.5 MPa $\sqrt{m}$) and σ_f (620 MPa) are achieved in 10 vol% $Ce_2Zr_2O_7$ composites which sinter to ~98% density. Such high values are usually achieved only with pressure assisted sintering of Al_2O_3 based composites other than Al_2O_3-ZrO_2 composites.

Acknowledgement

Partial support of this work by Council of Scientific And Industrial Research (CSIR), Govt. of India is gratefully acknowledged. Measurement of CTE by Dr. A. M. Umarjee of IISc Bangalore is also thankfully acknowledged.

References

1. P. F. BECHER and W. H. WARWICK, *J. Am. Ceram. Soc.* **77** (1994) 2689.
2. K. NIIHARA and A. NAKAHIRA, *Mater. Sci. Monogr.* **68** (1991) 637.
3. R. P. WAHI and B. ILSCHNER, *J. Mater. Sci.* **15** (1980) 875.
4. J. LIU and P. D. OWNBY, *J. Am. Ceram. Soc.* **74** (1991) 674.
5. T. N. TIEGS and P. F. BECHER, *Am. Ceram. Soc. Bull.* **66** (1987) 339.
6. J. HOMNEY, W. L. VAUGHN and M. K. FERBER, *ibid.* **67** (1987) 333.
7. G. C. WEI and P. F. BECHER, *Am. Ceram. Soc. Bull.* **64** (1985) 298.
8. Y. S. CHOU and D. J. GREEN, *J. Am. Ceram. Soc.* **76** (1993) 1985.
9. B. BUDIANSKY, J. W. HUTCHINSON and A. G. EVANS, *J. Mech. Phys. Solids* **34** (1986) 167.
10. S. MASCHIO, O. SBAIZERO and S. MERIANI, in "Euro Ceramics, Vol. 3," edited by G. de With, R. A. Terpstra and R. Metselaar (Elsevier Applied Science, 1989) p. 377.
11. F. F. LANGE, G. L. DUNLOP and B. I. DAVIS, *J. Am. Ceram. Soc.* **69** (1986) 237.
12. E. TANI, M. YOSHIMURA and S. SOMIYA, *ibid.* **66** (1983) 506.
13. M. YASHIMA, H. TAKASHINA, M. KALIKHANA and M. YOSHIMURA, *ibid.* **77** (1994) 1869.
14. P. DUWEZ and F. ODELL, *ibid.* **33** (1950) 274.
15. A. I. LEONOV, A. B. ANDREEVA and E. K. KELER, *Izv. Akad. Nauk. SSSR, Neorg. Mater.* **2** (1966) 137.
16. H. Y. ZHU, T. HIRATA and Y. MURAMATSU, *J. Am. Ceram. Soc.* **75** (1992) 2843.
17. A. SAHA, D. C. AGRAWAL and A. SHARMA, in "Ceramic Transactions, Vol. 38," edited by N. P. Bansal (American Ceramic Society, Westervillie, OH, 1994) p. 497.
18. S. BHATTACHARYYA and D. C. AGRAWAL, *J. Mater. Sci.* **30** (1995) 1495.
19. R. T. DEHOFF, ASTM STP No 430, American Society for Testing and Materials, Philadelphia, Pennsylvania, 1968, p. 63.
20. J. C. WURST and J. A. NELSON, *J. Am. Ceram. Soc.* **55** (1972) 109.
21. Powder Diffraction File, JCPDS Card No. 28–271.
22. K. T. FABER and A. G. EVANS, *Acta. Metall.* **31** (1983) 565.
23. B. BUDIANSKY, J. C. AMAZIGO and A. G. EVANS, *J. Mech. Phys. Solids* **36** (1988) 167.
24. N. CLAUSSEN, *J. Am. Ceram. Soc.* **59** (1976) 49.
25. M. TAYA, S. HAYASHI, A. S. KOBAYASHI and H. S. YOON, *ibid.* **73** (1990) 1382.
26. G. C. WEI and P. F. BECHER, *ibid.* **67** (1984) 571.
27. C. H. MCMURTRY, W. D. G. BOECKER, S. G. SESHADRI, J. S. ZANGHI and J. E. GARNIER, *Am. Ceram. Soc. Bull.* **66** (1987) 325.
28. M. A. JANNEY, *ibid.* **66** (1987) 322.
29. T. HANSSON, R. WARREN and J. WASEN, *J. Am. Ceram. Soc.* **76** (1993) 841.
30. P. L. SWANSON, C. J. FAIRBANKS, B. R. LAWN, Y. W. MAI and B. J. HOCKEY, *ibid.* **70** (1987) 279.
31. C. W. LI, S. C. LUI and J. GOLDACKER, *ibid.* **78** (1995) 449.
32. N. P. PADTURE, J. L. RUNYAN, S. J. BENNISON, L. M. BRAUN and B. R. LAWN, *ibid.* **76** (1993) 2241.
33. P. F. BECHER, K. B. ALEXANDER, A. BLEIER, S. B. WATERS and W. H. WARWICK, *ibid.* **76** (1993) 657.
34. A. SAWAGUCHI, K. TODA and K. NIIHARA, *ibid.* **74** (1991) 1142.

Received 28 January 1999
and accepted 3 February 2000